US009236072B1

(12) **United States Patent**
Lee

(10) **Patent No.: US 9,236,072 B1**
(45) **Date of Patent: Jan. 12, 2016**

(54) **SERVO CONTROL USING A MODEL OF TEMPERATURE-DEPENDENT FRICTION**

(71) Applicant: **Seagate Technology LLC**, Cupertino, CA (US)

(72) Inventor: **Ju-Il Lee**, Eden Prairie, MN (US)

(73) Assignee: **SEAGATE TECHNOLOGY LLC**, Cupertino, CA (US)

(*) Notice: Subject to any disclaimer, the term of this patent is extended or adjusted under 35 U.S.C. 154(b) by 0 days.

(21) Appl. No.: **14/736,731**

(22) Filed: **Jun. 11, 2015**

(51) **Int. Cl.**

G11B 5/596	(2006.01)
G11B 5/55	(2006.01)
G05B 13/04	(2006.01)

(52) **U.S. Cl.**
CPC ***G11B 5/5565*** (2013.01); ***G11B 5/5547*** (2013.01); ***G11B 5/5552*** (2013.01); *G05B 13/042* (2013.01)

(58) **Field of Classification Search**
None
See application file for complete search history.

(56) **References Cited**

U.S. PATENT DOCUMENTS

6,636,375	B1	10/2003	Ding et al.	
6,937,430	B2 *	8/2005	Ge	G11B 5/5565 318/561
7,440,225	B1	10/2008	Chen et al.	
8,442,692	B2	5/2013	Okitsu et al.	

FOREIGN PATENT DOCUMENTS

CN	201611867	U	10/2010

* cited by examiner

Primary Examiner — K. Wong
(74) *Attorney, Agent, or Firm* — Hollingsworth Davis, LLC

(57) **ABSTRACT**

A first friction coefficient that is modeled as affecting a rotational velocity of a voice coil motor is modified. A second friction coefficient that is modeled as affecting a rotational acceleration of the voice coil motor is also modified. The first and second friction coefficients change in response to a change in ambient temperature. A control effort used to control the voice coil motor is changed based on the modified first and second friction coefficients.

20 Claims, 11 Drawing Sheets

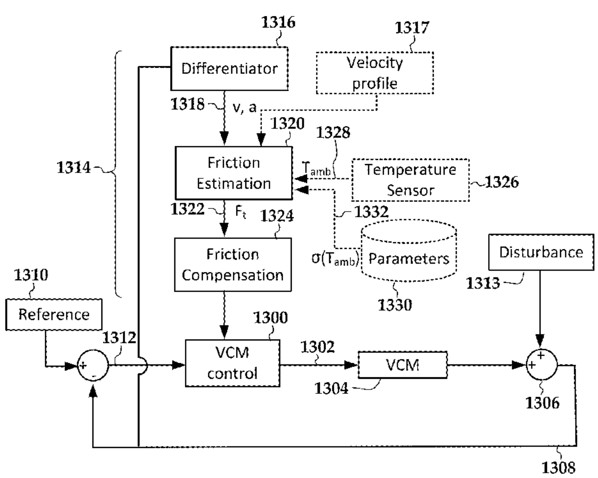

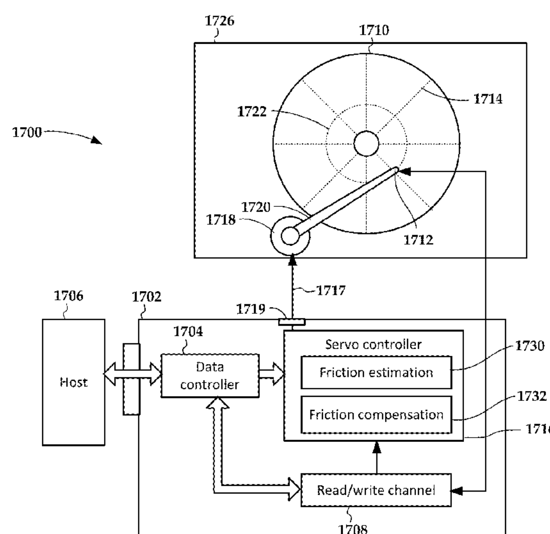

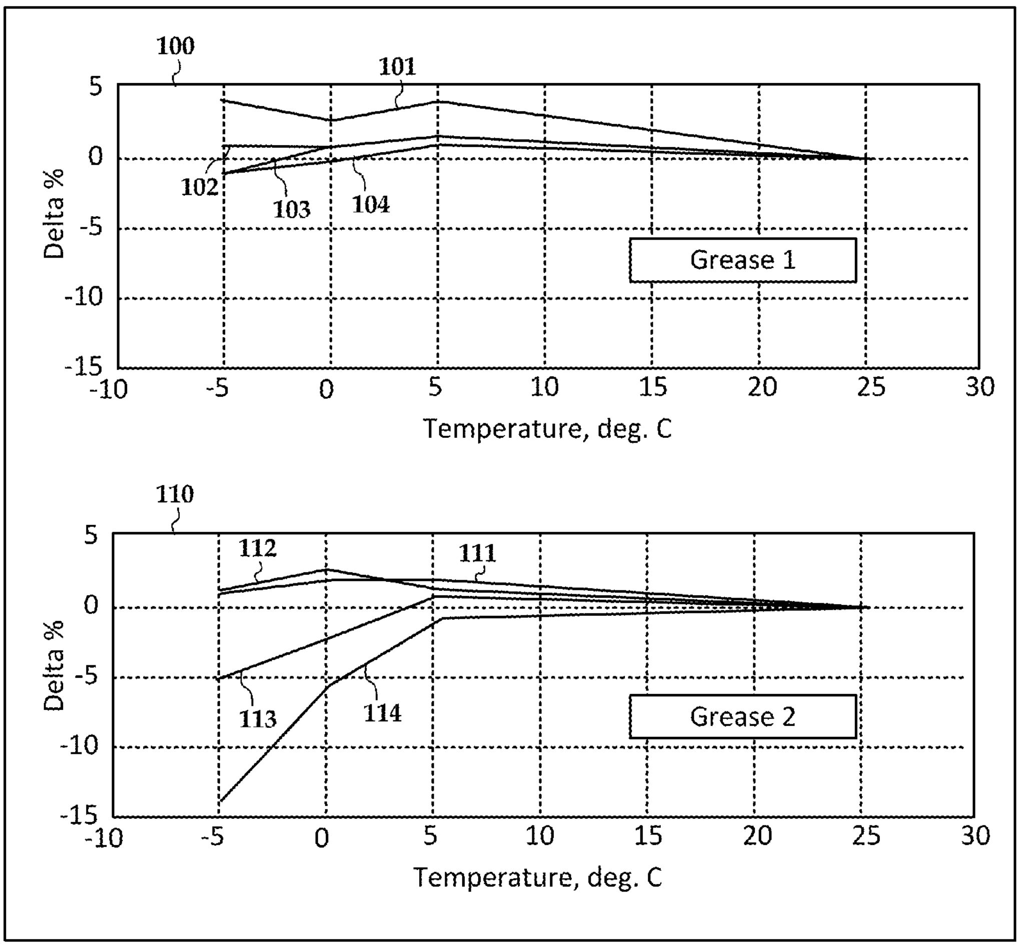
100
101
5
0
-5
-10
-15
Delta %
102
103
104
Grease 1
-10
-5
0
5
10
15
20
25
30
Temperature, deg. C
110
112
111
113
114
Grease 2
Temperature, deg. C

FIG. 1

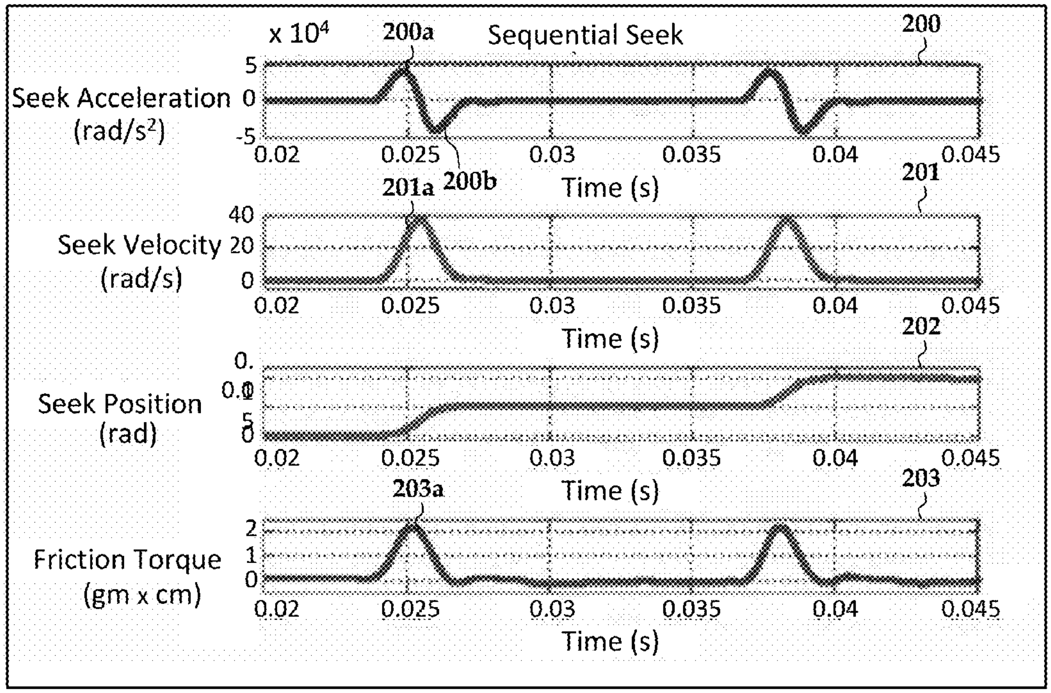
x 10^4
200a
Sequential Seek
200
Seek Acceleration (rad/s²)
5
0
-5
200b
Time (s)
201a
201
Seek Velocity (rad/s)
40
20
0
Time (s)
202
Seek Position (rad)
Time (s)
203a
203
Friction Torque (gm x cm)
2
1
0
Time (s)
0.02
0.025
0.03
0.035
0.04
0.045

FIG. 2

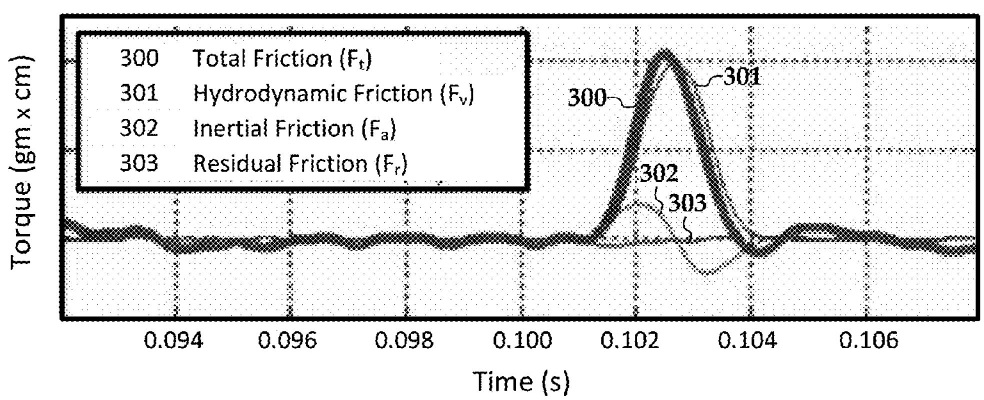
300 Total Friction (Ft)
301 Hydrodynamic Friction (Fv)
302 Inertial Friction (Fa)
303 Residual Friction (Fr)
300
301
302
303
Torque (gm x cm)
0.094
0.096
0.098
0.100
0.102
0.104
0.106
Time (s)

FIG. 3

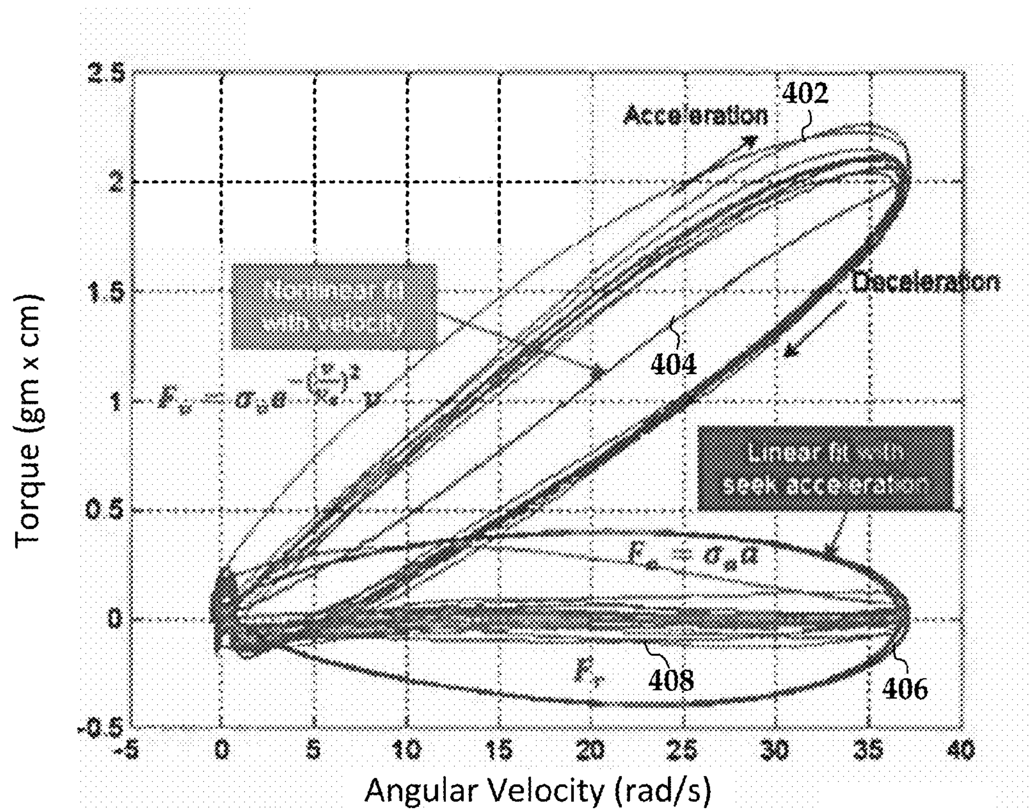
Acceleration
402
Deceleration
Nonlinear fit with velocity
404
Linear fit with seek acceleration
408
406
Torque (gm x cm)
Angular Velocity (rad/s)

FIG. 4

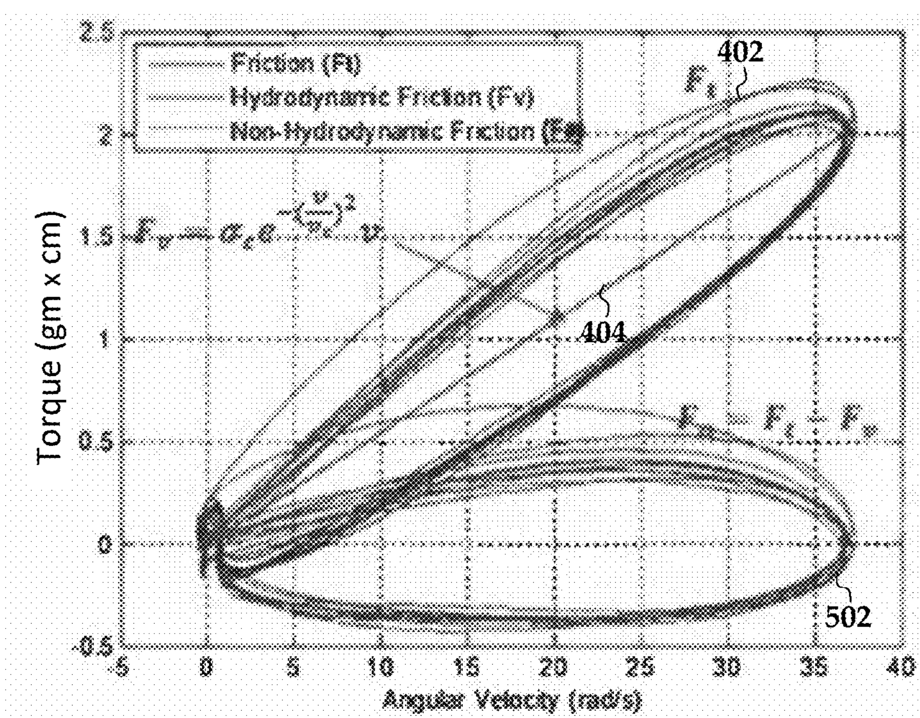
Friction (Ft)
Hydrodynamic Friction (Fv)
Non-Hydrodynamic Friction (Fa)
402
404
502
Torque (gm x cm)
Angular Velocity (rad/s)

FIG. 5

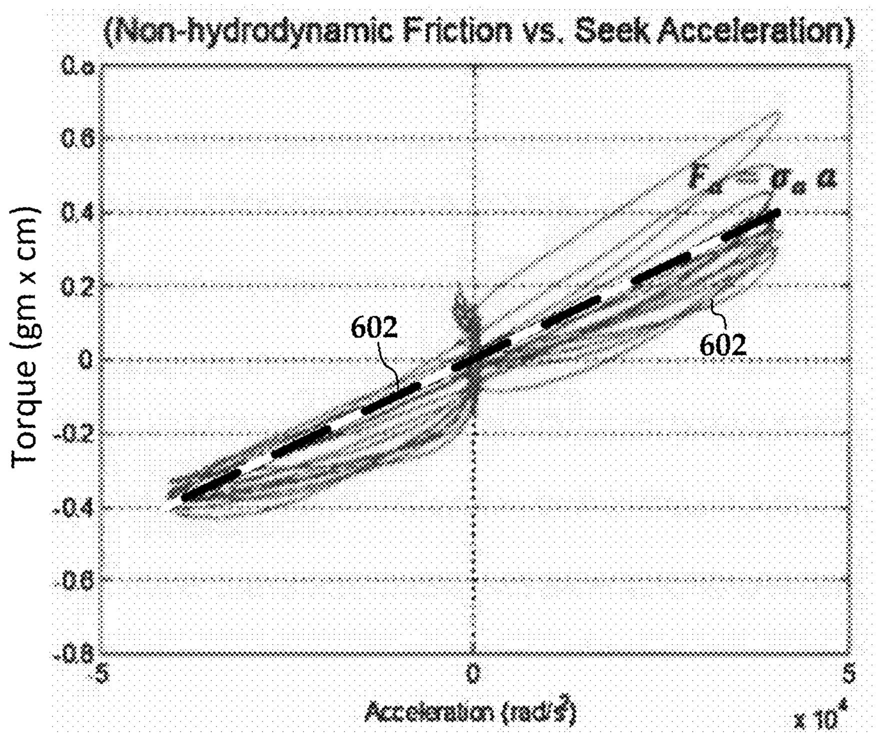
(Non-hydrodynamic Friction vs. Seek Acceleration)
0.8
0.6
0.4
0.2
0
-0.2
-0.4
-0.6
-0.8
Torque (gm x cm)
$F_a = \sigma_a a$
602
602
-5
0
5
Acceleration (rad/s²)
x 10⁴

FIG. 6

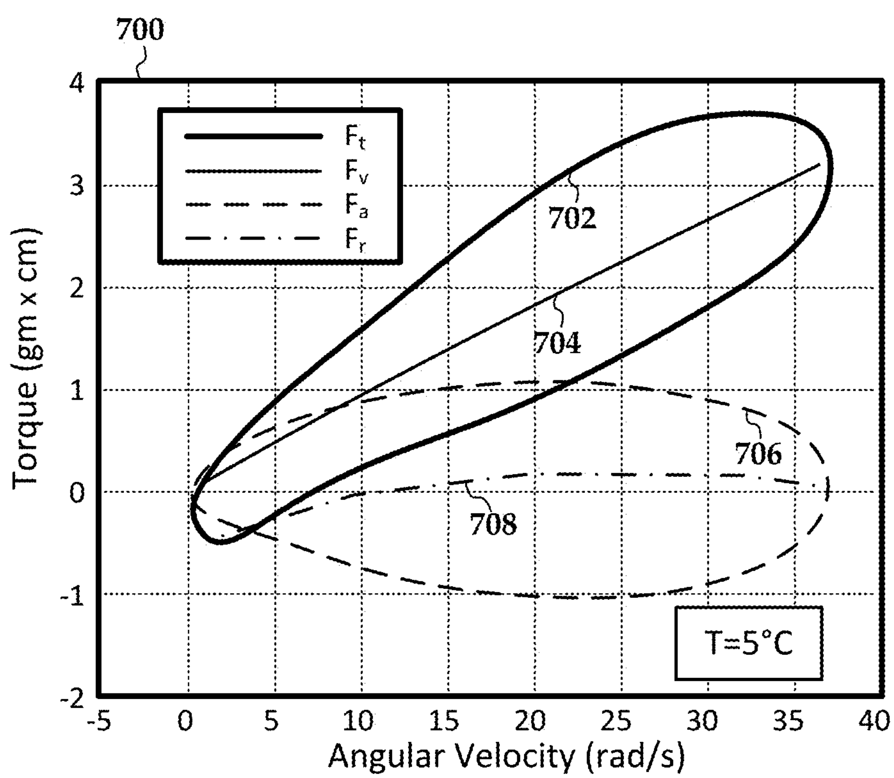
700
4
3
2
1
0
-1
-2
Torque (gm x cm)
F_t
F_v
F_a
F_r
702
704
706
708
T=5°C
-5
0
5
10
15
20
25
30
35
40
Angular Velocity (rad/s)

FIG. 7

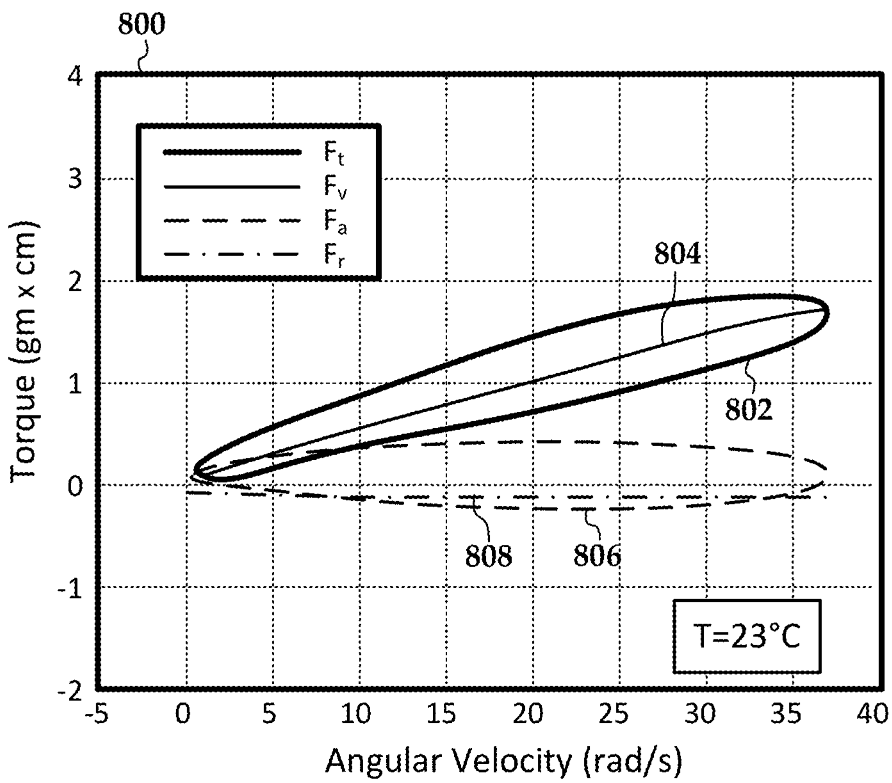
800
Torque (gm x cm)
Angular Velocity (rad/s)
F_t
F_v
F_a
F_r
804
802
808
806
T=23°C
4
3
2
1
0
-1
-2
-5
0
5
10
15
20
25
30
35
40

FIG. 8

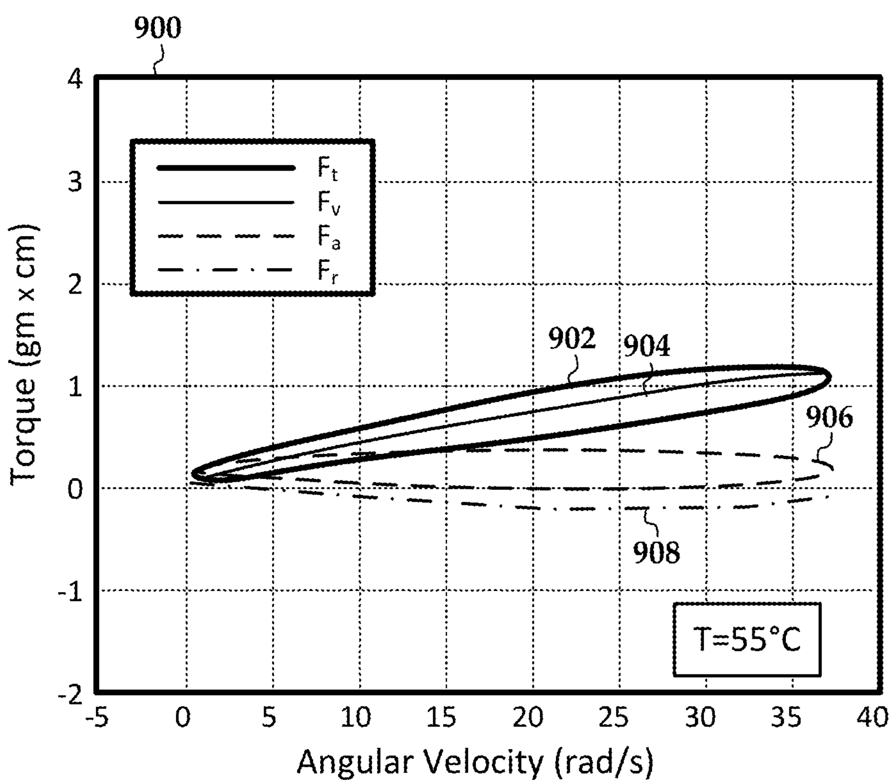
900
Torque (gm x cm)
Angular Velocity (rad/s)
F_t
F_v
F_a
F_r
902
904
906
908
T=55°C
4
3
2
1
0
-1
-2
-5
0
5
10
15
20
25
30
35
40

FIG. 9

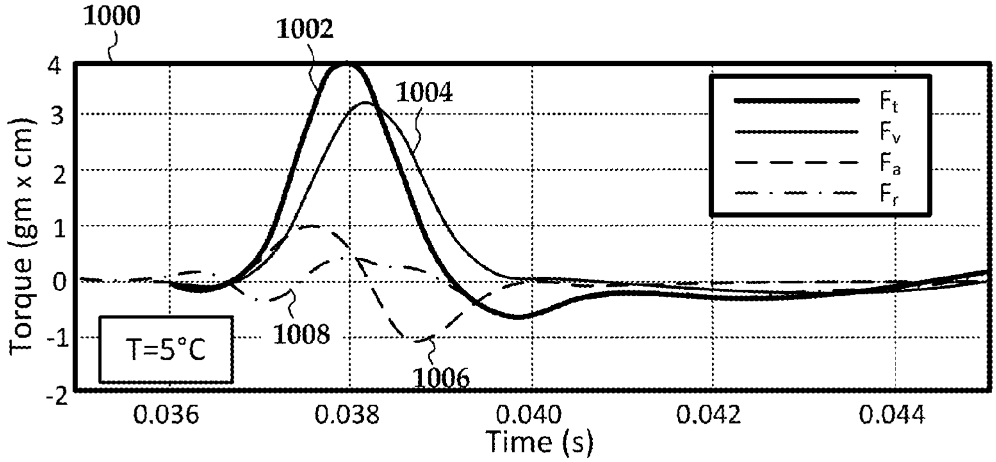

FIG. 10

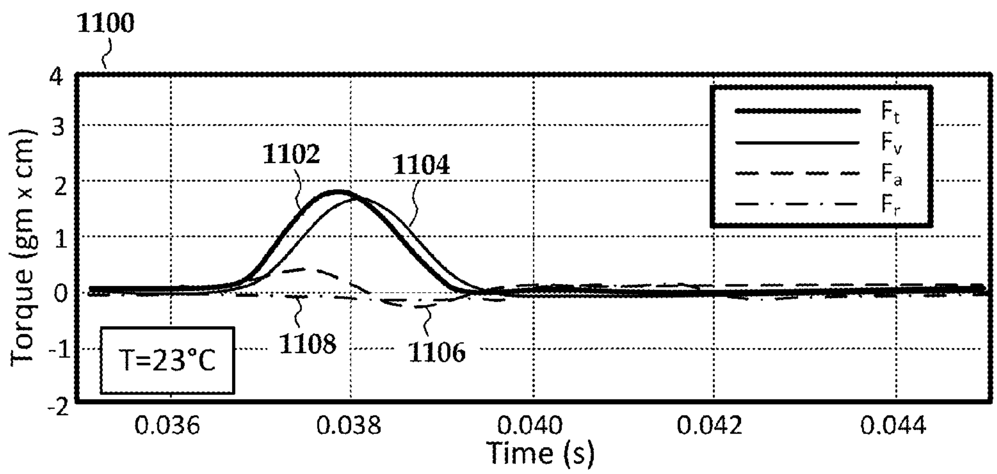

FIG. 11

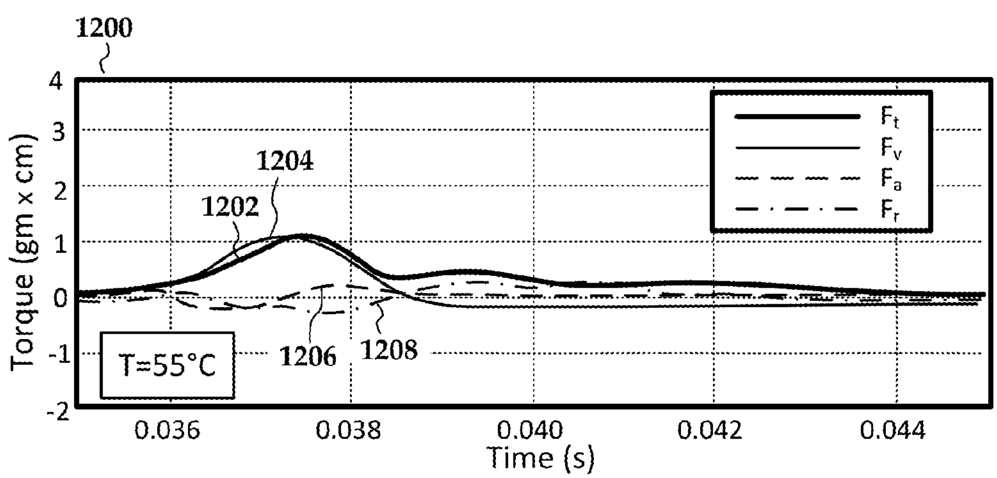

FIG. 12

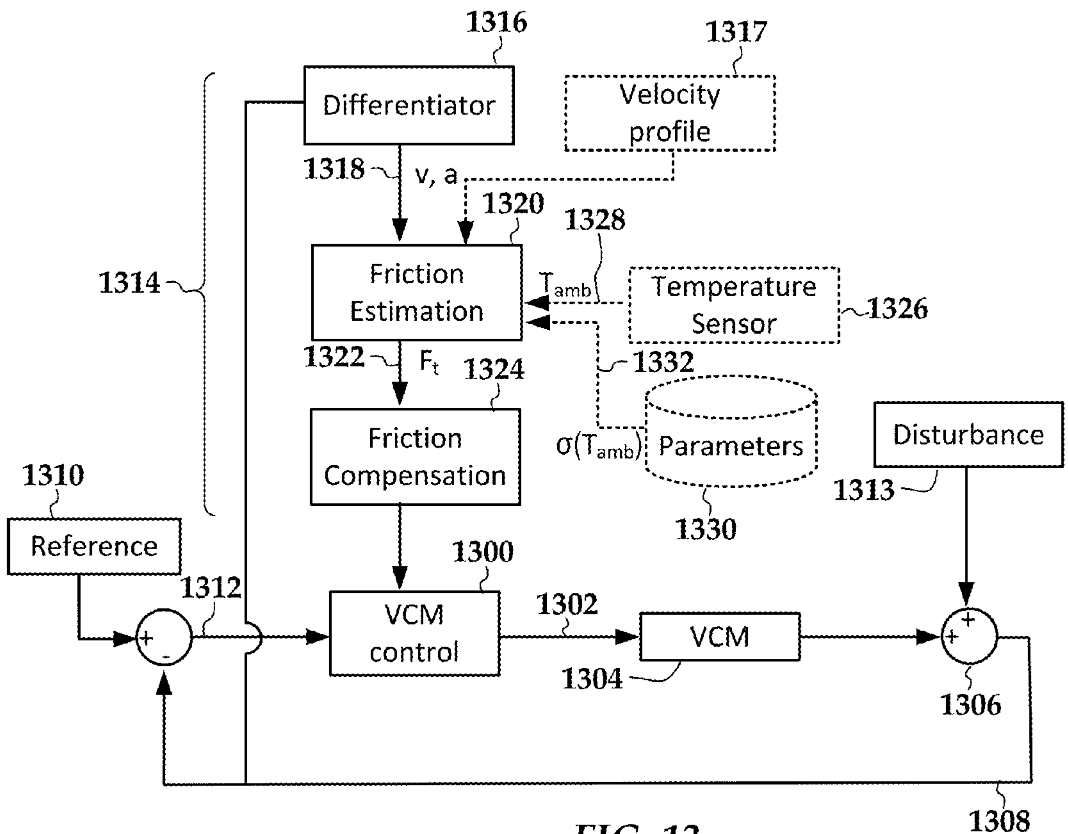
1316
Differentiator
1317
Velocity profile
1318
v, a
1320
1328
Friction Estimation
T_amb
Temperature Sensor
1326
1314
1322
F_t
1324
1332
Friction Compensation
σ(T_amb)
Parameters
Disturbance
1310
1313
1330
Reference
1300
1312
VCM control
1302
VCM
1304
1306
1308

FIG. 13

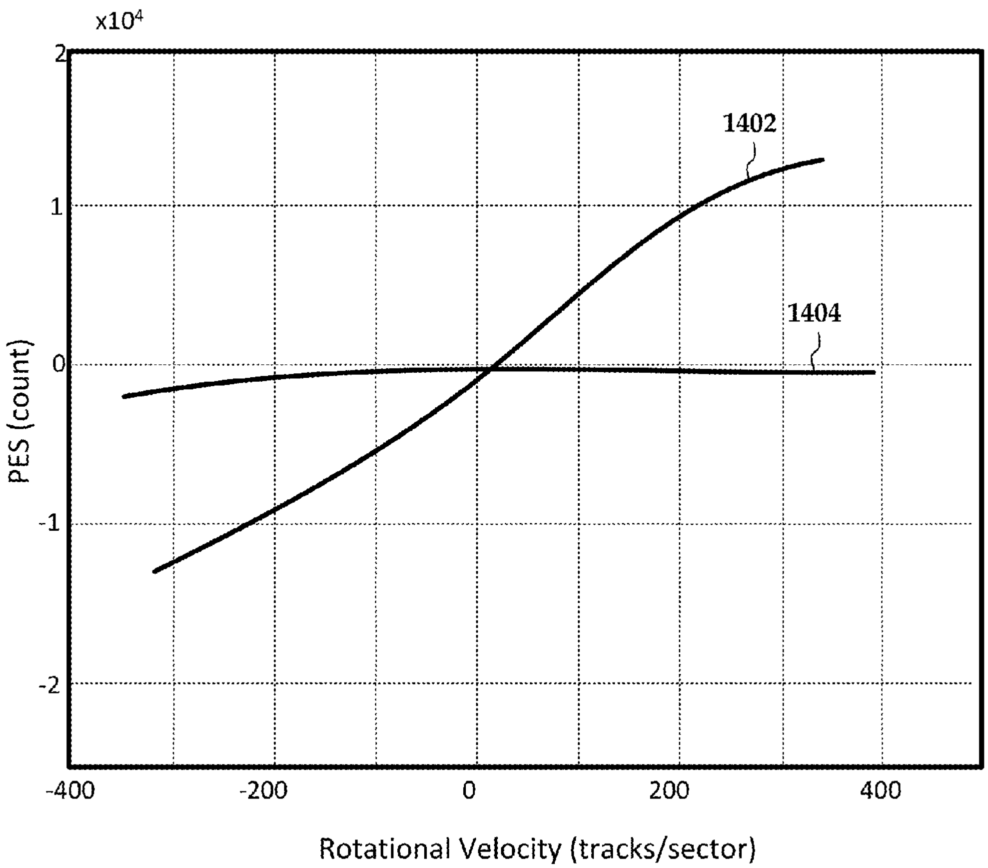
x10^4
2
1
0
-1
-2
PES (count)
-400
-200
0
200
400
Rotational Velocity (tracks/sector)
1402
1404

FIG. 14

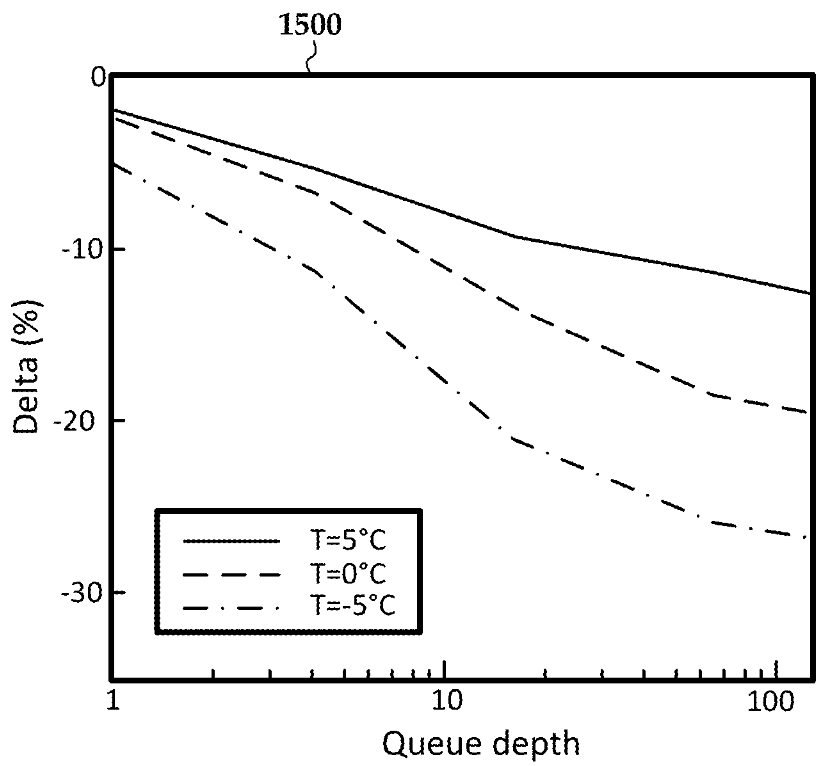
1500
0
-10
-20
-30
Delta (%)
1
10
100
Queue depth
T=5°C
T=0°C
T=-5°C

FIG. 15

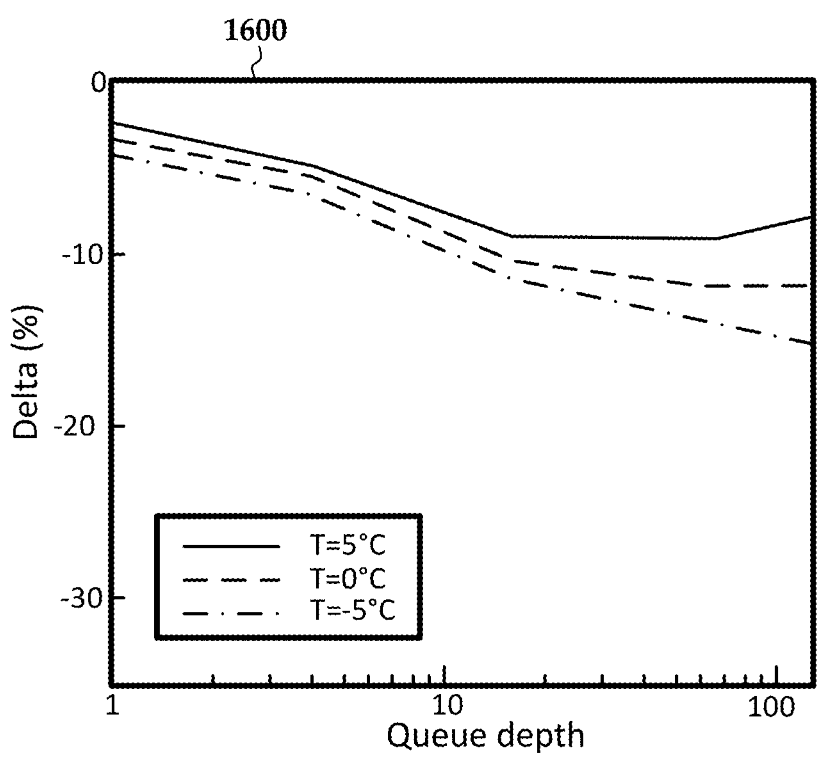
1600
0
-10
-20
-30
Delta (%)
1
10
100
Queue depth
T=5°C
T=0°C
T=-5°C

FIG. 16

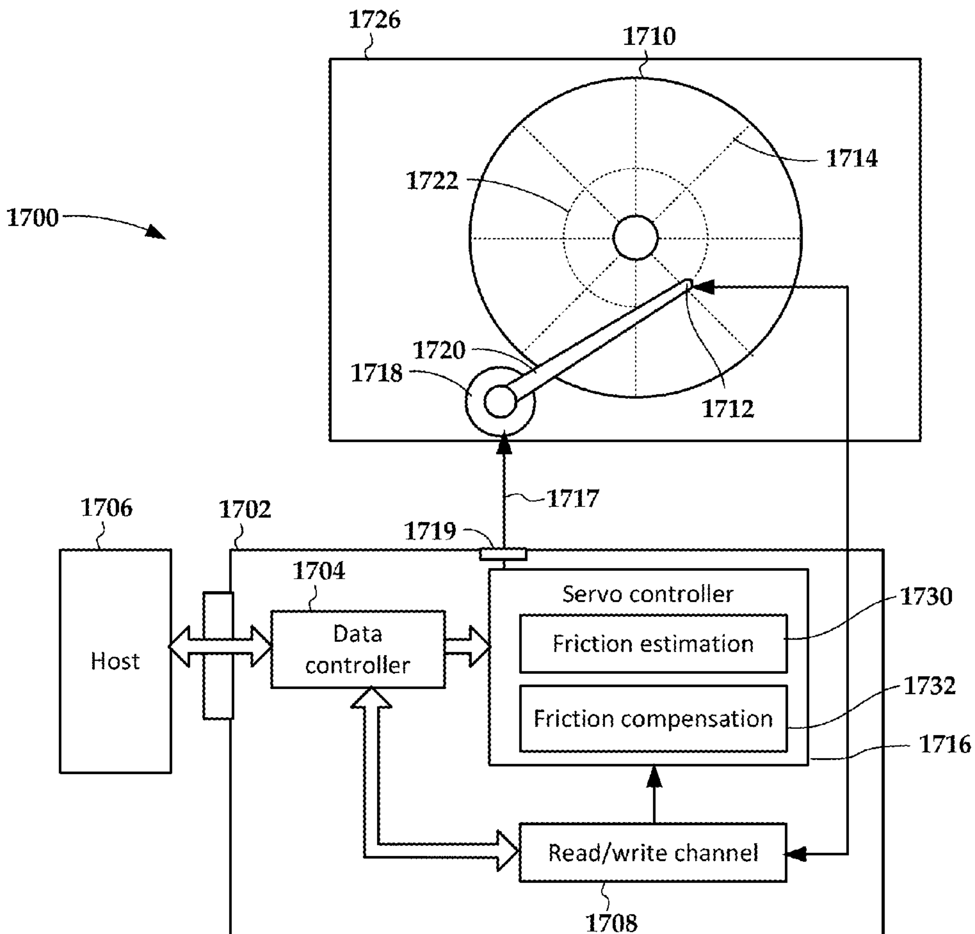
1726
1710
1714
1722
1700
1720
1718
1712
1717
1706
1702
1719
1704
Servo controller
1730
Host
Data controller
Friction estimation
1732
Friction compensation
1716
Read/write channel
1708

FIG. 17

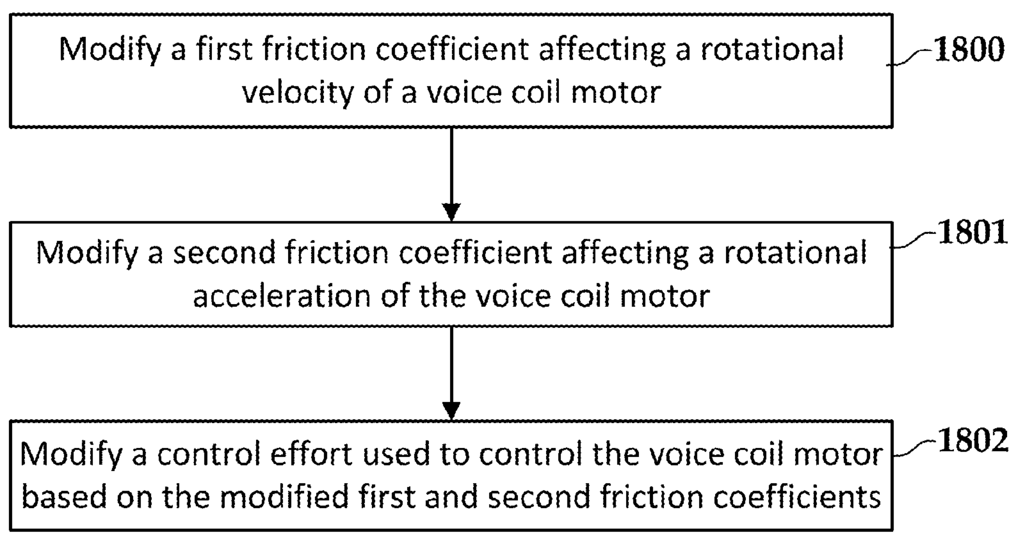
Modify a first friction coefficient affecting a rotational velocity of a voice coil motor
1800
Modify a second friction coefficient affecting a rotational acceleration of the voice coil motor
1801
Modify a control effort used to control the voice coil motor based on the modified first and second friction coefficients
1802

FIG. 18

SERVO CONTROL USING A MODEL OF TEMPERATURE-DEPENDENT FRICTION

SUMMARY

Various embodiments described herein are generally directed to servo control using a model of temperature-dependent friction. In one embodiment, a first friction coefficient that is modeled as affecting a rotational velocity of a voice coil motor is modified. A second friction coefficient that is modeled as affecting a rotational acceleration of the voice coil motor is also modified. The first and second friction coefficients change in response to a change in ambient temperature. A control effort used to control the voice coil motor is changed based on the modified first and second friction coefficients.

These and other features and aspects of various embodiments may be understood in view of the following detailed discussion and accompanying drawings.

BRIEF DESCRIPTION OF THE DRAWINGS

The discussion below makes reference to the following figures, wherein the same reference number may be used to identify the similar/same component in multiple figures.

FIG. **1** is a set of graphs showing effects of temperature on seek performance for different actuator greases used in a data storage device according to an example embodiment;

FIGS. **2** and **3** are graphs showing seek friction measurements according to an example embodiment;

FIGS. **4**, **5**, and **6** are graphs showing modeled components of friction as a function of rotational velocity according to an example embodiment;

FIGS. **7**, **8**, and **9** are graphs showing effects of temperature modeled components of friction as a function of rotational velocity according to example embodiments;

FIGS. **10**, **11**, and **12** are graphs showing effects of temperature modeled components of friction as a function of time according to example embodiments;

FIG. **13** is a control diagram of a servo control system according to an example embodiment;

FIGS. **14**, **15**, and **16** are graphs comparing temperature compensated and temperature uncompensated servo control according to example embodiments;

FIG. **17** is a block diagram of an apparatus according to an example embodiment; and

FIG. **18** is a flowchart showing a method according to an example embodiment.

DETAILED DESCRIPTION

Hard disk drives utilize actuators (e.g., voice coil motor) that position a read/write head over a disk surface. For example, a dual-stage actuator utilizes a voice coil motor that rotates an arm, a read/write head being positioned at the far end of the arm. The dual-stage actuator also includes a microactuator (e.g., piezo-actuator) that causes small displacements of the read/write head. A dual-stage servo control system generally uses the voice coil motor for large displacements (e.g., track seeks) and the microactuator for fine adjustments (e.g., track following).

The voice coil motor can have a significant influence on servo system performance during certain operations such as track seeks. For example, seek time can be the largest part of the total completion time for operations such as random read and writes. The present disclosure relates to issues that can affect bearing friction of voice coil motor, which can negatively impact seek performance of hard disk drives.

Friction from the actuator pivot bearing can adversely affect drive performance. While the servo system can compensate for friction within some predefined range, if the friction changes over time or under some environmental conditions, the effectiveness of servo compensation can decrease, leading to longer seek times. For example, it has been found that certain bearing grease can have a significant change in viscosity at low temperature, which can impact seek performance.

In FIG. **1**, a pair of graphs **100**, **110** illustrate how temperature can affect seek performance for different types of actuator bearing grease in equivalent data storage devices according to example embodiments. In graphs **100** and **110** the curves **101-104** and **111-114**, respectively, represent performance for instruction queue depth of 1, 4, 16, and 64, respectively. Generally, an instruction queue may act as a buffer between a system controller that processes storage commands (e.g., reads and writes) and a servo processor that moves the read/write head to fulfill the commands. When a large number of commands are queued up, the queue may be reordered to minimize the size of the seeks needed to fulfill the queued commands. Therefore, the seek distance may generally be inversely proportional to the queue depth. As such, issues that affect settling on a track will have relatively high impact for larger queue depth, and relatively less impact for small queue depth.

In graph **100**, the performance was obtained from data storage device used a lower molecular weight grease with the actuator pivot compared to the device in graph **110**, which used a higher molecular weight grease. The vertical axes of the graphs **100**, **110** represent a percentage of change in the number of input/output operations per second (IOPS) that the system was capable of performing relative to a 25° C. baseline. Expression (1) below shows how Delta (%) was obtained.

$$\text{Delta}(\%) = \frac{IOPS_{[T]} - IOPS_{[T=25C]}}{IOPS_{[T=25C]}} \times 100 \tag{1}$$

As indicated by comparing curves **104** and **114**, for example, the higher molecular weight grease results in a reduction in IOPS at low temperatures. This effect is more pronounced for the highest queue depth of 64 (curve **114**) because increased friction of the grease may increase the time it takes to locate and settle on a target track. Nonetheless, this higher molecular weight grease may have other advantages (e.g., reduced outgassing), and so example embodiments described below include features to compensate for the low temperature performance of higher molecular weight grease.

In reference now to FIG. **2**, graphs **200-203** illustrate additional details of seek performance of a disk drive device according to an example embodiment. The data in graphs **200-203** was measured during a series of 0.05 radian seeks in a representative disk drive device. In this device, a 0.05 sequential seek covers about 15 k to 25 k tracks. The data in graph **203** was obtained using a component-level dynamic bearing friction measurement apparatus.

Graph **202** shows the radial position for each of the two seeks. Graphs **201** and **200** respectively show the velocity and acceleration peaks associated with the seek operations. Note that for each seek, the acceleration curve exhibits a positive peak (e.g., peak **200**_a_) as the arm accelerates away from the current track and then a negative peak (e.g., peak **200**_b_) as the arm decelerates as it approaches the target track. As seen by the friction curve in graph **203**, the peaks (e.g., peak **203**a) closely resembles the velocity peaks (e.g., peak **201**a), although the peak **203**a is shifted in time slightly to the left relative to peak **201**a, indicating acceleration also contributed to the friction.

In view of the measurements shown in FIG. **2**, a servo control system is described that utilizes parametric friction model as shown below in Expressions (2)-(4) below. The total friction F_t in Expression (2) is the sum of: hydrodynamic friction F_v shown in Expression (3); inertial friction due to acceleration F_a shown in Expression (4); and residual friction F_r, which is due to other ball/grease motions and is relatively constant at least relative to velocity and acceleration. In Expression (3), v is velocity, v_c is a reference velocity, and σ_v is a friction coefficient. In Expression (4), a is acceleration and σ_a is a friction coefficient. The friction components F_t, F_v, F_a, and F_r are plotted in the respective time domain curves **300-303** in the graph of FIG. **3**.

$$F_t=F_v+F_a+F_r \quad (2)$$

$$F_v=\sigma_v e^{-\left(\frac{v}{v_c}\right)^2} v \quad (3)$$

$$F_a=\sigma_a a \quad (4)$$

In FIG. **4**, a graph of torque versus angular/rotational velocity shows how the various friction components are modeled. Trace **402** represents measurements of total friction affecting a bearing of a representative disk drive device. Trace **404** represents a non-linear fit of hydrodynamic friction from lubricant fluid according to Expression (3) above. The exponential nonlinearity accounts for a slight slope decrease at high velocities, which can be due to change in damping characteristics at high velocities where more lubricant is being forced into the ball/race interface. Trace **406** represents a linear fit of the resistant torque due to inertia from ball and/or lubricant fluid.

In FIG. **5**, a graph shows a trace **502** that results from subtracting the hydrodynamic friction **406** from the total friction **402** of FIG. **4**, both of which are reproduced in FIG. **5**. Curve **502** will also contain some components of residual friction. The similarities between curve fit **406** in FIG. **4** and curve **502** in FIG. **5** illustrate the correspondence between the measurements and the modeling of inertial friction according to Expression (4) above. In FIG. **6**, a graph shows the data of curve **502** plotted as a function of angular acceleration, resulting in trace **602**. Dashed line **604** is the linear fit of this data.

Referring back to FIG. **4**, trace **408** is the residual friction component, which is obtained by subtracting the fit of hydrodynamic friction **404** and the fit of inertial friction **406** from total friction **402**. The residual friction component **408** is relatively constant as a function of angular velocity. Generally, by decomposing seek-induced friction into three components (hydrodynamic/viscous, inertial, residual), an accurate model of temperature-dependent friction can be used in servo control. In FIGS. **7-9**, graphs illustrate the effects of temperature on the three different friction components.

In graphs **700**, **800**, **900** in FIGS. **7-9**, friction components analogous to those shown in FIG. **4** are plotted for ambient temperatures of 5° C., 23° C., and 55° C., respectively. Specifically, curves **702**, **802**, **902** represent an average total friction, curves **704**, **804**, **904** represent fits of hydrodynamic friction, curves **706**, **806**, **906** represent fits of inertial friction, and curves **708**, **808**, **908** represent averages of residual friction. Similarly, graphs **1000**, **1100**, **1200** in FIGS. **10-12** are time domain plots of the friction components shown in FIGS. **7-9** for the same ambient temperatures of 5° C., 23° C., and 55° C., respectively. Specifically, curves **1002**, **1102**, **1202** represent total friction, curves **1004**, **1104**, **1204** represent hydrodynamic friction, curves **1006**, **1106**, **1206** represent fits of inertial friction, and curves **1008**, **1108**, **1208** represent the resulting residual friction.

Based on the results shown in FIGS. **7-12**, it is apparent that, relative to 23° C., ambient temperature of 5° C. causes a significant increase in hydrodynamic friction (~70% in this example device) and inertial friction (~320% in this example device). For the 55° C. case, all friction components are reduced. This change in friction components can be shown numerically by comparing the values of parameters in Expressions (3) and (4). In Table 1 below, the relative values of these parameters, as well as an absolute value of residual friction F_r, are shown for each temperature.

TABLE 1

Parameter	T = 5° C.	T = 23° C.	T = 55° C.
σ_v	0.092	0.054	0.043
v_c	148	100	56
σ_a	25.9×10^{-6}	6.0×10^{-6}	-5.1×10^{-6}
$\|F_r\|$	0.159	0.073	0.108

In order to ensure consistent seek performance over a wide temperature range, a data storage device according to example embodiments may utilize a servo control system as shown in the block diagram of FIG. **13**. Generally, a controller **1300** provides control signals **1302** that drive a voice coil motor (VCM) **1304**. The VCM **1304** rotates in response to the control signal **1302**, causing a change in position **1306** of a read/write head. The read/write head may be influenced by exogenous disturbances **1313** (e.g., vibration) that also affects its position. A reference input **1310** is a command that drives the read/write head to a particular position. The difference between the reference command **1310** and actual position **1308** is defined as position error signal (PES) **1312**. The PES **1312** is fed back to the controller **1300**, and the system attempts to maintain a zero value of PES **1312** during steady state operations, e.g., tracking.

The servo control system includes a friction compensator **1314** that compensates for temperature-dependent changes to the VCM **1304**. A friction estimator **1320** estimates a current friction **1322** uses at least an estimation of rotational velocity and acceleration to estimate current friction **1322**. One way of estimating rotational velocity and acceleration is to use a differentiator **1316** that reads the position signal **1308** (e.g., PES **1312**) and provides an output **1318** that includes an estimation of rotational velocity v and rotational acceleration a. In the alternate, an estimate of velocity and acceleration may be obtained by other means, as indicated by velocity profile component **1317**. Generally, the velocity profile component **1317** can estimate velocity and acceleration by secondary measures such as time to traverse servo wedges. In such a case, a known seek profile (which includes time-dependent velocity and acceleration data) can be fit to conform to the measured times, thereby providing an estimate of velocity and acceleration.

A compensation module **1324** modifies operation of the VCM controller **1300** based on the friction estimate **1322** provided by the friction estimator **1322**. For example, the compensation module **1324** may alter various parameters (e.g., gain, skew rate, control effort) used by the VCM controller **1300** in order to ensure the VCM **1304** minimizes seek times. The compensation module **1324** may vary the amount of alteration/modification based on certain factors besides estimated friction **1322**, such as ambient temperature, queue-depth, etc. In another example, the compensation module **1324** may be configured as a feedforward compensator.

In one example, the friction estimator **1320** uses an adaptive estimation of viscous and inertial friction models, the adaptive estimation updating the various friction coefficients on a per-seek basis. For the viscous model, the relation shown in Expression (3) above is used to form the model as shown in Expressions (5) and (6) below. Adaptive gain $\sigma_v(k)$ is estimated for each seek number k and is obtained as shown in Expressions (7) and (8) below. Similarly, an inertial friction adaptive model for the relation shown in Expression (4) above substitutes $\sigma_a(k)$ for in σ_a with an adaptive gain shown in Expressions (9) and (10) below, where k again represents the seek number. In both Expressions (8) and (10), the summation of position error signal over v(j) is for velocities greater than $v_{threshold}$. Generally, this causes only relatively high velocity events to contribute to the adaptive parameter X_{avg}^{v}.

$$F_v=\sigma(v)\cdot v \tag{5}$$

$$\sigma(v)=\sigma_v(k)e^{-\left(\frac{v}{v_c}\right)^2} \tag{6}$$

$$\sigma_v(k+1)=\sigma_v(k)+\mu_v X_{avg}^{v}(k) \tag{7}$$

$$X_{avg}^{v}(k)=\frac{1}{N}\sum_{|v(j)|>v_{threshold}} PES(j)\cdot\mathrm{sign}(v(j)) \tag{8}$$

$$\sigma_a(k+1)=\sigma_a(k)+\mu_a X_{avg}^{a}(k) \tag{9}$$

$$X_{avg}^{a}(k)=\frac{1}{N}\sum_{|v(j)|>v_{threshold}} PES(j)\cdot\mathrm{sign}(a(j)) \tag{10}$$

The adaptive friction models described above do not require express measurements of temperature in order to operate. However, such a system may make use of such measurements instead of an adaptive model, and/or use such measurements as an alternate during initialization, safe mode, alternate control mode, etc. As shown in FIG. **13**, a temperature sensor **1326** may be utilized to determine current ambient temperature **1328**. A database **1330** may store temperature-dependent friction parameters **1332**, which may be used as shown in Expressions (2)-(4) to estimate total friction. The temperature dependent friction parameters **1332** may be specific to a particular device, varying based on such factors as voice coil motor, voice coil motor lubricant/grease, number of arms and read/write heads, etc.

It will be understood that a servo system such as shown in FIG. **13** may include additional actuators (e.g., microactuators) and control components (e.g., disturbance compensation) that are not illustrated, and the illustrated friction compensation features may be applicable to servo systems that also include such features. For example, if the servo system is implemented as a multiple-stage controller, additional components (e.g., filters, plant models) may be used to determine separate contributions that different actuator stages velocity have on position **1308** in order to model velocity and acceleration that affect the VCM **1304** only.

In FIGS. **14-16**, graphs illustrate results of using adaptive friction compensation on a disk drive device according to an example embodiment. In FIG. **14**, a graph compares position error (PES) during random seeks for friction-compensated servo control (curve **1404**) and uncompensated servo control (curve **1402**) at 10° C. ambient temperature. This improvement is most evident for high queue depth seeks. In FIGS. **15** and **16**, graphs **1500**, **1600** illustrate change in IOPS versus queue depth for uncompensated device (graph **1500**) and friction-compensated device (graph **1600**). In both cases, the Delta (%) is determined as in Expression (1) above. For a maximum queue depth of 128, the delta of graph **1500** is −13%, −20%, and −27% for ambient temperatures of 5° C., 0° C., and 15° C., respectively. The delta of graph **1600** at maximum queue depth is −8%, −12%, and −15% for ambient temperatures of 5° C., 0° C., and 15° C., respectively.

While the friction-compensating servo control systems described above may be used in any positioning application, various features are described in the context of a hard disk drive. In FIG. **17**, a block diagram illustrates a control logic circuit **1702** of a hard disk drive apparatus **1700** according to an example embodiment. The circuitry **1702** includes a data controller **1704** that processes read and write commands and associated data from a host device **1706**. The host device **1706** may include any electronic device that can be communicatively coupled to store and retrieve data from a data storage device, e.g., a computer. The data controller **1704** is coupled to a read/write channel **1708** that reads from and writes to a surface of a magnetic disk **1710**.

The read/write channel **1708** generally converts data between the digital signals processed by the data controller **1704** and the analog signals conducted through one or more read/write heads **1712** during read operations. To facilitate the read operations, the read/write channel **1708** may include analog and digital circuitry such as preamplifiers, filters, decoders, digital-to-analog converters, timing-correction units, etc. The read/write channel **1708** also provides servo data read from servo wedges **1714** on the magnetic disk **1710** to a servo controller **1716**. The servo controller **1716** uses these signals to provide a voice coil motor control signal **1717** to a VCM **1718**. The control signals **1717** are processed (e.g., converted from digital-to-analog, amplified, filtered, etc.) via control interface circuitry **1719** that is coupled to the servo controller **1716**. In response to the control signal **1717**, the VCM **1718** rotates an arm **1720** upon which the read/write heads **1712** are mounted.

Data within the servo wedges **1714** is used to detect the location of a read/write head **1712** relative to the magnetic disk **1710**. The servo controller **1716** uses servo data to move a read/write head **1712** to an addressed track **1722** and block on the magnetic disk **1710** in response to the read/write commands (seek mode). While data is being written to and/or read from the disk **1710**, the servo data is also used to maintain the read/write head **1712** aligned with the track **1722** (track following mode).

The movement of the read/write head **1412** can be affected by temperature-dependent friction affecting the VCM **1718**. To counter the effects of this friction, a friction estimation module **1730** estimates inertial and hydrodynamic friction affecting the VCM **1718**. A friction compensation module **1732** modifies the servo performance based on the estimated friction. For example, the friction estimation module **1730** may modify a first friction coefficient affecting a rotational velocity of the VCM **1718** and a second friction coefficient of a rotational acceleration of the VCM **1718**, the first and second friction coefficients changing in response to a change in ambient temperature. The friction compensation module **1732** modifies a control effort used to control the VCM **1718** based on the modified first and second friction coefficients.

Although two separate controllers **1704** and **1716** and a read write channel **1708** have been shown for purposes of illustration, it is to be understood that their functionality described herein may be integrated within a common integrated circuit package or distributed among more than one integrated circuit package. Similarly, a head disk assembly can include a plurality of data storage disks **1710**, an actuator arm **1720** with a plurality of read/write heads **1712** (or other sensors) which are moved radially across different data storage surfaces of the disk(s) **1710** by the actuator motor **1718** (e.g., voice coil motor), and a spindle motor (not shown) which rotates the disk(s) **1710**.

In FIG. **18**, a flowchart illustrates a method according to an example embodiment. The method involves modifying **1800** a first friction coefficient affecting a rotational velocity of a voice coil motor and a modifying **1801** a second friction coefficient affecting a rotational acceleration of the voice coil motor. The first and second friction coefficients change in response to a change in ambient temperature. A control effort used to control the voice coil motor is modified **1802** based on the modified first and second friction coefficients.

Unless otherwise indicated, all numbers expressing feature sizes, amounts, and physical properties used in the specification and claims are to be understood as being modified in all instances by the term "about." Accordingly, unless indicated to the contrary, the numerical parameters set forth in the foregoing specification and attached claims are approximations that can vary depending upon the desired properties sought to be obtained by those skilled in the art utilizing the teachings disclosed herein.

The various embodiments described above may be implemented using circuitry, firmware, and/or software modules that interact to provide particular results. One of skill in the arts can readily implement such described functionality, either at a modular level or as a whole, using knowledge generally known in the art. For example, the flowcharts and control diagrams illustrated herein may be used to create computer-readable instructions/code for execution by a processor. Such instructions may be stored on a non-transitory computer-readable medium and transferred to the processor for execution as is known in the art. The structures and procedures shown above are only a representative example of embodiments that can be used to provide the functions described hereinabove.

The foregoing description of the example embodiments has been presented for the purposes of illustration and description. It is not intended to be exhaustive or to limit the invention to the precise form disclosed. Many modifications and variations are possible in light of the above teaching. Any or all features of the disclosed embodiments can be applied individually or in any combination are not meant to be limiting, but purely illustrative. It is intended that the scope of the invention be limited not with this detailed description, but rather determined by the claims appended hereto.

What is claimed is:

1. A method, comprising:

modifying a first friction coefficient that is modeled as affecting a rotational velocity of a voice coil motor and a second friction coefficient that is modeled as affecting a rotational acceleration of the voice coil motor, the first and second friction coefficients changing in response to a change in ambient temperature; and

modifying a control effort used to control the voice coil motor based on the modified first and second friction coefficients.

2. The method of claim **1**, wherein the first friction coefficient comprises a non-linear function of the rotational velocity.

3. The method of claim **2**, wherein the first coefficient comprises an exponential function.

4. The method of claim **3**, wherein the first coefficient is of the form

$$\sigma_v e^{-\left(\frac{v}{v_c}\right)^2}.$$

5. The method of claim **1**, wherein modifying the first and second friction coefficients comprises adaptively changing the first and second friction coefficients on a per-seek basis.

6. The method of claim **1**, wherein modifying the first and second friction coefficients comprises determining adaptive parameters X_{avg}^{v} and X_{avg}^{a} that are both based on a summation of position error signal values for previous seeks.

7. The method of claim **6**, wherein the summation of the position error signal values is performed only for seek velocities that exceed a threshold.

8. The method of claim **1**, wherein the first and second friction coefficients change in response to a bearing grease of the voice coil motor, properties of the bearing grease changing in response to the change in ambient temperature.

9. An apparatus, comprising:

control interface circuitry that processes signals sent to a voice coil motor; and

a servo controller coupled to the control interface circuitry and configured to:

modify a first friction coefficient that is modeled as affecting a rotational velocity of the voice coil motor and a second friction coefficient that is modeled as affecting a rotational acceleration of the voice coil motor, the first and second friction coefficients changing in response to a change in ambient temperature; and

modify a control effort used to control the voice coil motor based on the modified first and second friction coefficients.

10. The apparatus of claim **9**, wherein the first friction coefficient comprises a non-linear function of the rotational velocity.

11. The apparatus of claim **10**, wherein the first coefficient comprises an exponential function.

12. The apparatus of claim **11**, wherein the first coefficient is of the form

$$\sigma_v e^{-\left(\frac{v}{v_c}\right)^2}.$$

13. The apparatus of claim **9**, wherein modifying the first and second friction coefficients comprises determining adaptive parameters X_{avg}^{v} and X_{avg}^{a} that are both based on a summation of position error signal values for previous seeks.

14. The apparatus of claim **13**, wherein the summation of the position error signal values is performed only for seek velocities that exceed a threshold.

15. The apparatus of claim **10**, wherein the first and second friction coefficients changing change in response to a bearing grease of the voice coil motor, properties of the bearing grease changing in response to the change in ambient temperature.

16. An apparatus, comprising:

control interface circuitry that processes signals sent to a voice coil motor; and

a servo controller coupled to the control interface circuitry and comprising:

a friction estimator configured to adaptively determine a temperature-dependent friction affecting the voice coil motor, the temperature-dependent friction determined based on a first friction coefficient that is modeled as affecting a rotational velocity of the voice coil motor and a second friction coefficient that is modeled as affecting a rotational acceleration of the voice coil motor, the first friction coefficient comprising a non-linear function of the rotational acceleration; and

a friction compensator configured to modify a control effort used to control the voice coil motor based on the temperature-dependent friction.

17. The apparatus of claim **16**, wherein the first coefficient comprises an exponential function.

18. The apparatus of claim **17**, wherein the first coefficient is of the form

$$\sigma_v e^{-\left(\frac{v}{v_c}\right)^2}.$$

19. The apparatus of claim **16**, wherein the first and second friction coefficients are determined based on adaptive parameters X_{avg}^{v} and X_{avg}^{a} that are both determined from a summation of position error signal values for previous seeks.

20. The apparatus of claim **19**, wherein the summation of the position error signal values is performed only for seek velocities that exceed a threshold.

* * * * *